Colloid Polym Sci (2008) 286:365–376
DOI 10.1007/s00396-007-1776-8

ORIGINAL CONTRIBUTION

# Structural and dynamical characterization of poly-gamma-glutamic acid-based cross-linked nanoparticles

**Judit Éva Fleischer Radu · Levente Novak · John F. Hartmann · Neda Beheshti · Anna-Lena Kjøniksen · Bo Nyström · János Borbély**

Received: 14 June 2007 / Revised: 6 August 2007 / Accepted: 4 September 2007 / Published online: 22 October 2007


**Abstract** This work describes the formation of water-soluble hydrophilic nanoparticles from biosynthetic poly-γ-glutamic acid (PGA). Nanoparticles were formed by cross-linking using 2,2′-(ethylenedioxy) diethylamine in the presence of water-soluble carbodiimide. The structure was determined by nuclear magnetic resonance spectroscopy and the particle size by transmission electron microscopy (TEM), size exclusion chromatography (SEC), and dynamic light-scattering (DLS) measurements. The results from TEM, SEC, and DLS reveal that the particle size depends on the ratio of cross-linking. Particle size values measured by TEM were between 20 and 90 nm. Formation of cross-linked nanoparticles results in a dramatic viscosity drop compared to the viscosity of the corresponding solution of the parent PGA. The viscosity and DLS experiments disclose an intriguing interplay between intrachain and interchain cross-linking of the polymer chains, depending on the cross-linker density and polymer concentration. The SEC measurements show that the retention time of the major portion of particles increase because of the higher cross-linking ratio. At moderate cross-linker concentration, intramolecular cross-linking is the dominant process, whereas at higher cross-linker densities, the interpolymer cross-linking plays an important role. As a result, large clusters are also formed.

**Keywords** Poly-gamma-glutamic acid · Nanoparticles · Cross-linking · DLS · Rheology

J. É. F. Radu · L. Novak · J. Borbély (✉)
Department of Colloid and Environmental Chemistry,
University of Debrecen,
4010 Debrecen, Hungary
e-mail: jborbely@delfin.unideb.hu

J. F. Hartmann
ElizaNor Polymer LLC,
Princeton Junction,
Princeton, NJ 08550, USA

N. Beheshti · A.-L. Kjøniksen · B. Nyström
Department of Chemistry, University of Oslo,
P.O. Box 1033, Blindern N-0315,
Oslo, Norway

J. Borbély
BBS Nanotechnology,
4225 Debrecen, P.O. Box 12, Hungary

## Introduction

Biomacromolecules, biodegradable polymers as biomaterials have an important role in fabrication of medical devices and in drug delivery systems [1]. The most valuable properties of these biopolymers are their biocompatibility and biodegradability [2].

The bacterially synthesized water-soluble poly-γ-glutamic acid (PGA) was discovered as a capsule of *Bacillus anthracis* in 1937 [3], which plays a role in antibiotic resistance and immune evasion [4] and later as a fermentation product that is freely secreted into the growth medium by several other *Bacilli*, most notably *B. subtilis* [5, 6] and *B. licheniformis* [7]. PGA consists of repetitive glutamic acid units connected by amide linkages between α-amino and γ-carboxylic acid functional groups (Fig. 1). The secondary structure of PGA has been described [8] as α-helix in an aqueous solution.

The naturally produced polymers may have molecular weights up to 1 million and usually contain nearly equal amounts of D- and L-units. The ratio of the two optical isomers can partially be controlled by technological means so that polymers with varying degree of stereoregularity can be made [9]. PGA is different from other proteins, in that

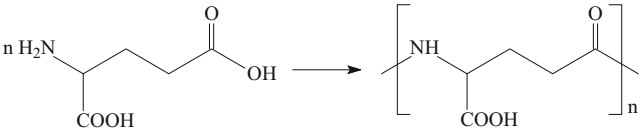


**Fig. 1** Chemical structure of PGA

glutamate is polymerized via the γ-amide linkages and thus is synthesized in a ribosome-independent manner. The location of genes responsible for PGA synthesis is a matter of controversy: They were reported to be present in the genomic deoxyribonucleic acid [10, 11], while other groups suggested they are carried in plasmids [12, 13]. Hydrolytic and enzymatic degradation of PGA gels has been demonstrated [14–17]. Several biomedical applications of PGA have been reported as drug carriers [18, 19] and bioadhesives [20].

PGA can easily be modified chemically through the free carboxyl groups [21–23]. Ester derivatives of PGA have been investigated for their capability to form biodegradable fibers and films that can replace the currently used nonbiodegradable polymers [24–25]. PGA and its derivatives have already been utilized as thickeners, humectants [26], and sustained-release materials, as well as drug carriers with high biodegradability in food, cosmetics industries, and in medicine [27, 28]. A problem with aqueous solutions of long-chain polyelectrolytes is the high viscosity of the solution even at low polymer concentrations, and the viscosity is usually sensitive to changes in pH and salt concentration [29, 30]. These effects make it difficult to modulate the properties of the system in a controlled manner.

In this work, we demonstrate that PGA can easily be cross-linked by amidation through the free carboxylic groups. The intrapolymer cross-linking process yields hydrophilic nanoparticles of PGA (PGANPs), which are significantly more compact than the analogous linear PGA and have different dynamical and rheological features than solutions of the parent PGA polymer. These PGANPs can provide a high specific surface for loading drugs, covalently conjugate antibodies, and other targeting molecules for biomedical applications. The aim of this study is to characterize these nanoparticles under various conditions of salinity, cross-linker density, and particle concentration. The competition between intrachain and interchain cross-linking in these samples is discussed. This knowledge about the system will help us to tailor-make the properties of these particles for different applications.

## Experimental section

### Materials

PGA ($M_w = 1.2 \times 10^6$) was prepared in our laboratory by using the biosynthetic methods. For the cross-linking, the used reagents (analytical grade) 2,2′-(ethylenedioxy)*bis* (ethylamine) (EDBEA) and 1-(3-(dimethylamino)propyl)-3-ethyl-carbodiimide hydrochloride) (CDI) were purchased from Sigma-Aldrich, Hungary. Disodium hydrogenophosphate, sodium dihydrogenphosphate, and sodium chloride (for the SEC eluent) were obtained from Sigma-Aldrich. Amberlite 15 (macroreticular cation-exchange resin in $H^+$ form) was bought from Sigma-Aldrich. Unless otherwise stated, other chemicals, for example, some of the constituents of the culture media, were of analytical grade and were purchased from REANAL, Budapest, Hungary.

### Preparation of PGA

PGA was produced from *Bacillus licheniformis*, strain ATCC 9945a [31], which was maintained on 1.5% (w/v) Bouillon agar slants [32] to produce appropriate cultivation conditions. The purification and isolation of PGA were carried out in the following way. PGA was precipitated by the addition of one and a half volume of acetone to the filtrate. The PGA was redissolved in water, dialyzed against distilled water, and freeze dried. Because the product is very hygroscopic and is in fact composed of free PGA acid (PGA-H) and sodium salt of PGA (PGA-Na) in an unknown ratio (with possibly some higher valence cations bound to the carboxylic groups), part of the PGA was further purified and converted to the free acid form by treatment with ion-exchange resin. 100 g of Amberlite 15 (macroreticular cation-exchange resin in $H^+$ form) was mixed with 5 l of partially purified PGA in solution and stirred for 30 min at room temperature. After decantation, PGA solution was mixed again with a new batch of resin, and the process was repeated twice. The resulting PGA-H solution is acidic (pH is approximately 2.8) and has a much lower viscosity than the initial PGA-Na–PGA-H mixture. Anions from the fermentation medium were removed by dialysis against distilled water for 7 days. Subsequent freeze drying for 3 days yielded pure PGA-H, which is practically not hygroscopic.

### Preparation of hydrophilic PGANPs

In the present study, PGA was cross-linked with EDBEA (see Scheme 1). Reaction takes place in water in the presence of a water-soluble carbodiimide (CDI). The cross-linking was performed in different proportions, such as 10, 25, 50, and 100% relative to the carboxylic groups of PGA (Table 1). All the reactions were carried out with 100 mg PGA dissolved in 10 ml of distilled water. The pH of the PGA solution was adjusted to 4.5 by adding 2 M NaOH, and then CDI dissolved in 1 ml water was added. The reaction mixture was cooled at 0 °C and stirred by a magnetic bar. EDBEA dissolved in 1 ml water was added

**Scheme 1** Formation of intramolecular cross-linking of PGA with EDBEA

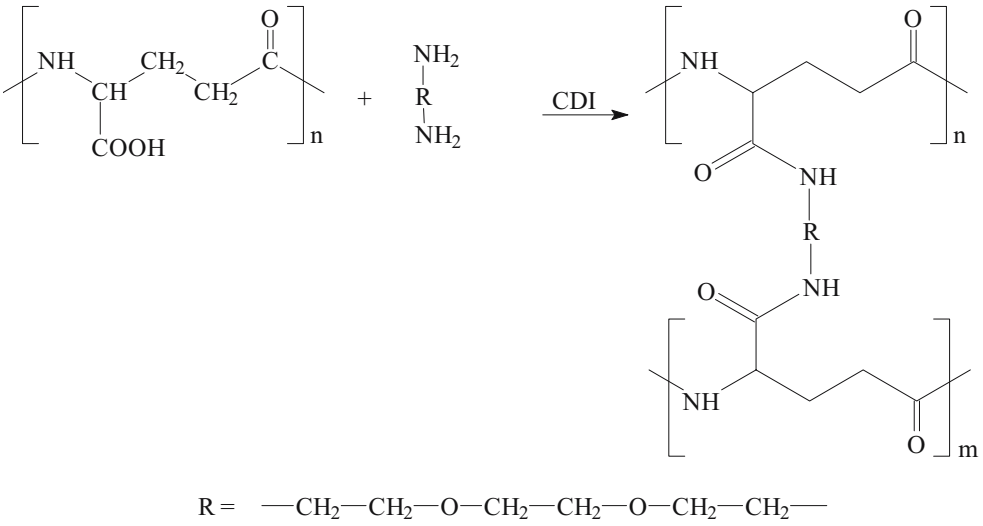


R = —$CH_2$—$CH_2$—O—$CH_2$—$CH_2$—O—$CH_2$—$CH_2$—

dropwise. After 24 h, the reaction mixture was placed in a dialysis bag of 10 kDa molecular weight cutoff and dialyzed against distilled water for 7 days and finally lyophilized.

## Characterization

*Infrared (ATR Fourier transform infrared) measurements* Infrared (IR) experiments were run by attenuate total reflexion (ATR) mode on a Perkin Elmer Spectrum 2000 instrument, combined with an IR microscope equipped with a single-reflexion Micro-ATR accessory and detector. The IR spectra were collected in the wavelength range of 4,000 to 650 $cm^{-1}$. Instrumental resolution was 1 $cm^{-1}$. IR experiments proved the formation of amide bond between the amine group of cross-linker and the carboxylic group of PGA (Fig. 2). Significant bands are: $\nu$ = 1,722 $cm^{-1}$(COOH), $\nu$ = 1,627 $cm^{-1}$(CO), and $\nu$ = 1,538 $cm^{-1}$ (Amide I).

*NMR spectroscopy* PGA and its derivatives were characterized structurally with NMR spectroscopy. $^1$H nuclear magnetic resonance (NMR) and $^{13}$C NMR spectra were obtained on Bruker 200SY (200 MHz) and Bruker DRX500 (500 MHz), respectively. The samples were dissolved in dimethyl sulfoxide (DMSO)-$d_6$ and in $D_2O$, and the chemical shifts are represented in parts per million (ppm) based on the signal for sodium 3-(trimethylsilyl)-propionate-$d_4$ as a reference.

**Table 1** Amounts of components for the cross-linking reactions of PGA

| Degree of cross-linking (%) | EDBEA (μl) | CDI (mg) |
|---|---|---|
| 10 | 6 | 23 |
| 25 | 15 | 57 |
| 50 | 30 | 115 |
| 100 | 60 | 230 |

*Size exclusion chromatography* Chromatographical analysis of PGA and its derivatives was performed on a Waters Ultrahydrogel Linear (300 × 7.8 mm) aqueous size exclusion chromatography (SEC) column mounted on a Hewlett-Packard HP1090 ChemStation high-performance liquid chromatography unit. The effluent was monitored at 220 nm. The eluent contained 140 mmol of NaCl, 7.5 mmol of $Na_2HPO_4$, and 5 mmol $NaH_2PO_4$ per liter of double-distilled water. Analyses were run at 40 °C with a flow rate of 0.7 ml/min. Low polydispersity molecular weight standards (sodium salt of linear polyacrylic acid, Fluka, Sigma-Aldrich, Budapest), and samples were dissolved in the eluent at concentrations between 0.01 and 0.5 g/l. Generally, apparent molecular weight corresponding to the elution peak apex ($M_p'$) was used to characterize the PGANPs.

*Transmission electron microscopy* The mean size of the PGANPs at dry conditions was measured with JEOL 2000 FX-II transmission electron microscope. Samples were prepared from the freeze-dried PGANPs, dissolved at a concentration of 10 μg/ml in distilled water, and then sonicated for 5 min to produce better particle dispersion on the copper grid. The sample for transmission electron microscopy (TEM) analysis was obtained by placing 20 μl of the solution containing the PGA nanoparticles onto a carbon-coated copper grid. It was dried at room temperature and then examined using TEM without any further modification or coating.

*Rheology* Steady-shear viscosity measurements were conducted in a Paar-Physica MCR 300 rheometer using a cone-

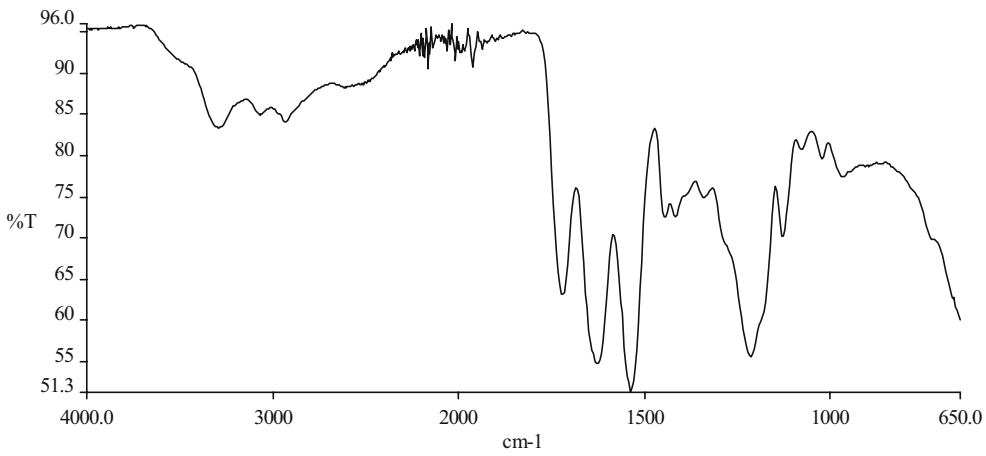


**Fig. 2** IR spectrum of PGANPs (25% cross-linking)

and-plate geometry, with a cone angle of 1° and a diameter of 75 mm. The samples were introduced carefully onto the plate, and to prevent evaporation of the solvent, the free surface of the sample was always covered with a thin layer of low-viscosity silicone oil (the viscoelastic response of the samples is not observed to be affected by this layer). The measuring cell is equipped with a temperature unit (Peltier plate) that provides an accurate temperature control (±0.05 °C) over an extended time. The shear viscosity measurements were conducted over an extended shear rate range.

*Dynamic light scattering* The beam from an argon ion laser (Lexel laser, model 95), operating at 514.5 nm with vertically polarized light, was focused onto the sample cell through a temperature-controlled chamber (temperature controlled to within ±0.05 °C) filled with refractive-index-matching silicone oil. The sample solutions were filtered through 5-μm filters (Millipore) directly into precleaned 10 mm NMR tubes (Wilmad Glass) of highest quality.

The light-scattering process defines a wave vector $q = (4\pi n/\lambda)\sin(\theta/2)$, where $\theta$ is the scattering angle and $n$ is the refractive index of the medium. The value of $n$ was determined for all samples at $\lambda$ = 514.5 nm by employing an Abbé refractometer.

In the present study, the full homodyne intensity autocorrelation function $g^2(t)$ was mostly measured at a scattering angle of 90° with an ALV-5000 multiple-τ digital correlator. If the scattered field obeys Gaussian statistics (as for all the solutions considered in this study), the measured correlation function $g^2(t)$ can be related to the theoretically amenable first-order electric field correlation function $g^1(t)$ by the Siegert relationship $g^2(t) = 1 + B\left|g^1(t)\right|$, where $B$ is an instrumental parameter. The correlation functions were recorded in the real time "multiple-τ"mode of the correlator, in which 256 time channels are logarithmically spaced over an interval ranging from 0.2 μs to almost 1 h. Experiment duration was in the range of 30–60 min.

Despite the fairly low concentrations of the PGA nanoparticles employed in this work, the decays of the correlation functions were always found to be bimodal [33–35] initially a single exponential, followed at longer times by a stretched exponential:

$$g^1(t) = A_f \exp(-t/\tau_f) + A_s \exp\left[-(t/\tau_{se})^{\beta}\right] \quad (1)$$

with $A_f + A_s = 1$. The parameters $A_f$ and $A_s$ are the amplitudes for the fast and the slow relaxation mode, respectively. Analyses of the time correlation functions of the concentration fluctuations in the domain $qR_h < 1$ ($R_h$ is the hydrodynamic radius) have shown [33–36] that the first term (short-time behavior) on the right-hand side of Eq. 1 is related to the mutual diffusion coefficient $D_m$ ($\tau_f^{-1} = D_m q^2$). In this study, the solutions probably consist of single particles and more or less aggregates depending on the cross-linking conditions under which the particles have been prepared. The fast relaxation mode monitors the diffusion of single particles and some small clusters of particles. In this work, the second term (long-time feature) is also found to be diffusive, and this slow relaxation mode is expected to be associated with the diffusion of larger aggregates. The variable $\tau_{se}$ is some effective relaxation time, and β ($0 < \beta \leq 1$) is a measure of the width of the distribution of relaxation times. The distribution of relaxation times for the present systems display values of β in the range β = 0.7–0.9. The mean relaxation time is given by

$$\tau_s = \frac{\tau_{se}}{\beta}\Gamma\left(\frac{1}{\beta}\right) \quad (2)$$

where $\Gamma(\beta^{-1})$ is the gamma function of $\beta^{-1}$.

In the analysis of the correlation function data, a nonlinear-fitting algorithm (a modified Levenberg–Marquardt method) was used to obtain best-fit values of the parameters $A_f$, $\tau_f$, $\tau_{se}$, and β appearing on the right-hand side of Eq. 1.

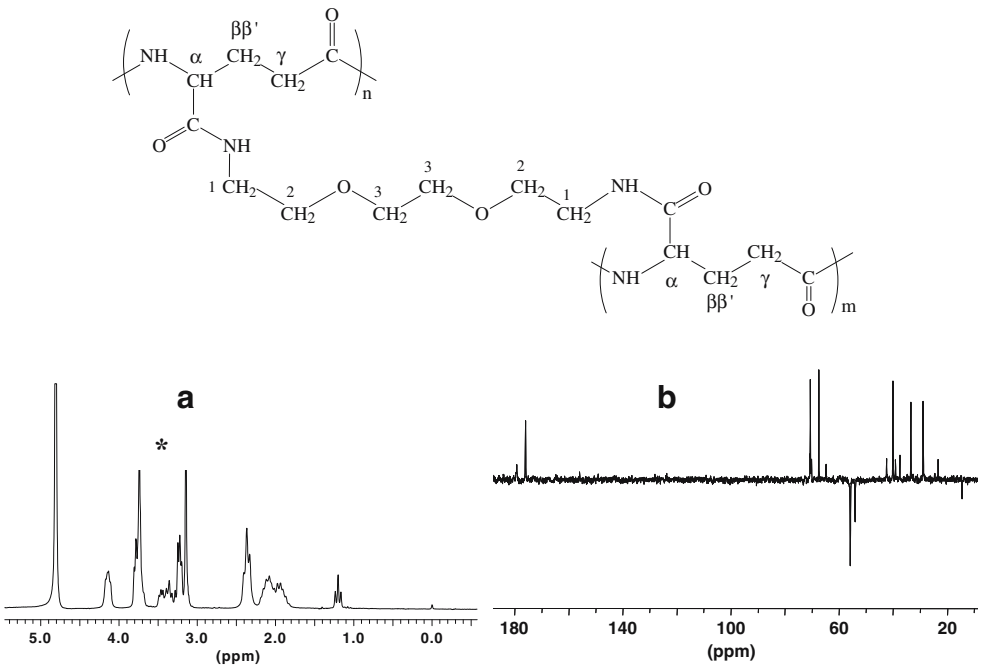


**Fig. 3** **a**,[1]H 200-MHz and **b** [13]C 50-MHz NMR spectra of 25% cross-linked PGANP in $D_2O$ solution at a 20 mg/ml concentration (*asterisk* indicates impurities)

## Results and discussion

*NMR results* The structure of PGA used for the synthesis and the obtained cross-linked nanosystems were characterized by NMR spectroscopy. The assignments and chemical shifts of the [1]H and [13]C signals of PGA and all PGANPs were determined. The [1]H chemical shifts of PGA are given as follows: (in DMSO-$d_6$): $\delta$ = 1.95 and 2.05 ppm (β and β′-$CH_2$), δ = 2.32 ppm (γ-$CH_2$), δ = 4.07 ppm (α-CH), δ = 8.07 ppm (NH); [13]C chemical shifts of PGA are (in $D_2O$): $\delta$ = 28.49 ppm (ββ′-$CH_2$), δ = 33.08 ppm (γ-$CH_2$), δ = 55.55 ppm (α-CH), δ = 175.77 and 179.02 ppm (CO groups).

[1]H and [13]C NMR chemical shifts of cross-linked PGANPs (Fig. 3) were assigned according to the [1]H and [13]C NMR spectra of PGA and EDBEA. The assignments and chemical shifts of PGANPs are given as follows: [1]H NMR ($D_2O$): $\delta$ = 1.90 and 2.10 ppm (β and β′-$CH_2$), $\delta$ =

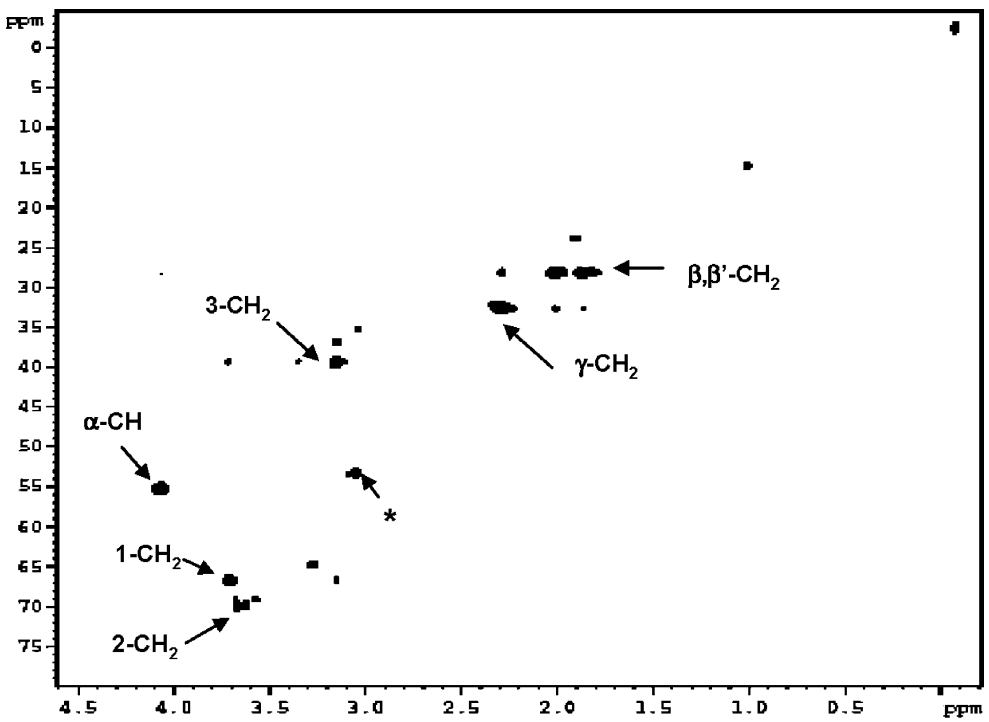


**Fig. 4** [1]H–[13]C HSQC 500-MHz NMR map of 25% cross-linked PGANP (*asterisk* indicates impurities)

2.45 ppm ($\gamma$-$CH_2$), $\delta$ = 4.15 ppm ($\alpha$-CH) of the PGA backbone and, $\delta$ = 3.22 ppm (3-$CH_2$), $\delta$ = 3.75 ppm (2-$CH_2$), ), and $\delta$ = 3.78 ppm (1-$CH_2$) for the cross-linker moiety. $^{13}$C NMR ($D_2O$): $\delta$ = 27.73 ppm ($\beta\beta'$-$CH_2$), $\delta$ = 32.56 ppm ($\gamma$-$CH_2$), $\delta$ = 39.70 ppm (3-$CH_2$), $\delta$ = 54.09 ppm ($\alpha$-CH), $\delta$ = 67.07 ppm (1-$CH_2$), $\delta$ = 70.23 ppm (2-$CH_2$), $\delta$ = 175.63–178.76 ppm (CO groups).

Figure 4 shows the $^1$H–$^{13}$C hetero single-quantum correlation spectrum (HSQC; 500 MHz) of PGANPs cross-linked at 25% with EDBEA. The chemical shifts were assigned according the $^{13}$C 50-MHz and $^1$H 200-MHz NMR spectra in $D_2O$.

The ratio of cross-linking was measured on the basis of the proton NMR spectra. The average integral values of the $\alpha$-CH, $\beta$ and $\beta'$-$CH_2$, and $\gamma$-$CH_2$ groups were compared to the integral values of the 3-$CH_2$ and 2-$CH_2$ groups of the cross-linker. The cross-linking ratios measured and calculated on the basis of stoichiometry are summarized in Table 2. We note that the experimental and calculated values of the cross-linking ratios and the molecular weights are in good agreement. The small deviation is explained with minor side reaction caused by rearrangement of the carbodiimide applied and the experimental errors of NMR integral values.

The cross-linking ratio was calculated on the base of the ratio of NMR integral values of $\alpha$-CH peak at $\delta$ = 4.25 ppm of PGA and 1-$CH_2$ at $\delta$ = 3.75 ppm. The observed cross-linking ratios were observed to be closed to the corresponding theoretical values. Theoretical molecular weight was calculated on the basis of the condensation reaction, anticipating 100% efficiency of the cross-linking reaction. The reported molecular weight values were calculated in accordance of slightly lower conversation values obtained from $^1$H NMR results. It is important to note that the overall molecular weight of PGANPs is higher in comparison to that of the starting PGA because the cross-linker molecules are incorporated.

*Molecular weight determination by SEC* SEC is generally used to determine the molecular weight (and molecular weight distribution) of polymers in solution. However, this is based on the assumption that the analyte and the standards used for the molecular weight calibration behave similarly in solution. Thus, the retention volume of a polymer is directly proportional to its hydrodynamic volume (or radius) and not to its molecular weight. PGA is a linear homopolymer, which presumably forms a random-coil structure in aqueous media, while its derivatives are cross-linked heteropolymers, with more or less restricted segment mobility. This implies that all molecular weight

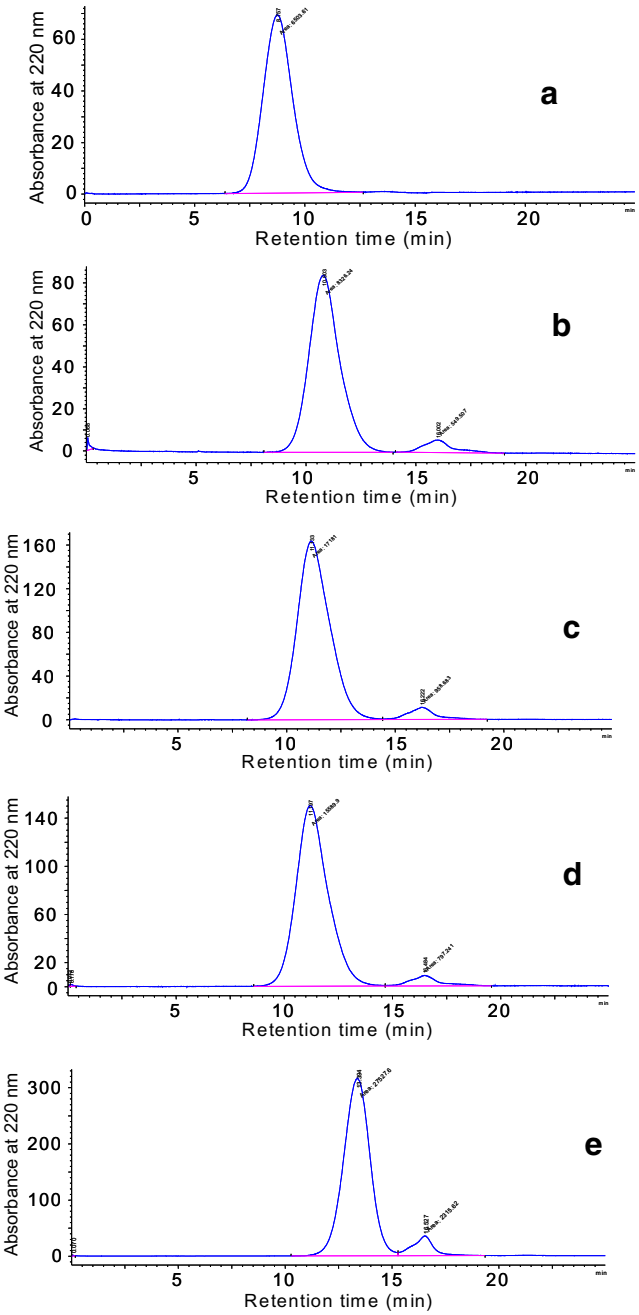


**Fig. 5** SEC traces of PGA and PGANPs. **a** PGA (Rt=8.757 min); **b** 10% cross-linked (Rt=10.803 min); **c** 25% cross-linked (Rt=11.133 min); **d** 50% cross-linked (Rt=11.197 min), and **e** 100% cross-linked (Rt=13.394 min). Experimental conditions as described above

**Table 2** Cross-linking ratios calculated and measured by NMR

| Sample | Theoretical cross-linking ratio (%) | Observed cross-linking ratio (%) | Theoretical tMw (kDa) | Observed oMw (kDa) |
|---|---|---|---|---|
| PGA | 0 | 0 | 890 | 890 |
| PGANP | 10 | 9±2 | 928 | 925±2% |
| PGANP | 25 | 25±3 | 987 | 987±3% |
| PGANP | 50 | 49±4 | 1,080 | 1,064±4% |
| PGANP | 100 | 98±6 | 1,277 | 1,255±6% |

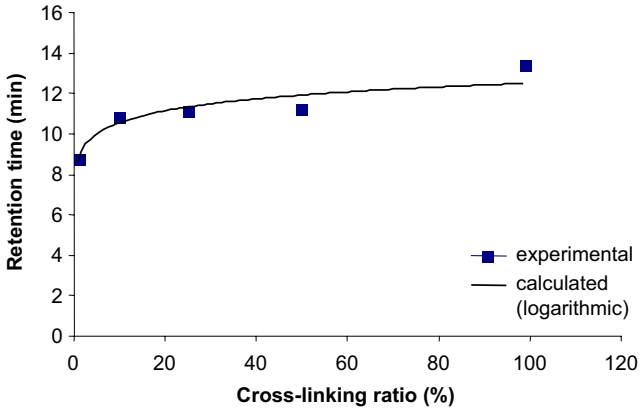


**Fig. 6** Plot of the retention time versus the cross-linking ratio, together with the calculated curve

values measured by SEC are in fact apparent molecular weights ($M'$), relative to the standard used (linear polyacrylic acid in our case). This implies that the "conventional" $M_w$ and $M_n$ values are somewhat misleading in the case of cross-linked products; therefore, only peak apex apparent molecular weight ($M'_p$) values will be provided.

The value of $M'_p$ of raw PGA did not change during the fermentation and was typically around or above $1 \times 10^6$. Purified PGA used for subsequent coupling reactions had a $M'_p$ of $8.9 \times 10^5$ ($M'_w = 1.03 \times 10^6$ and $M'_n = 4.2 \times 10^5$, and $M'_w/M'_n = 2.4$), while the cation-exchanger resin-treated PGA free acid (PGA-H) had a much lower molecular weight ($M'_p = 3.0 \times 10^5$), which possibly arose from acid-catalyzed degradation of the polymer by the resin or during the extensive dialysis.

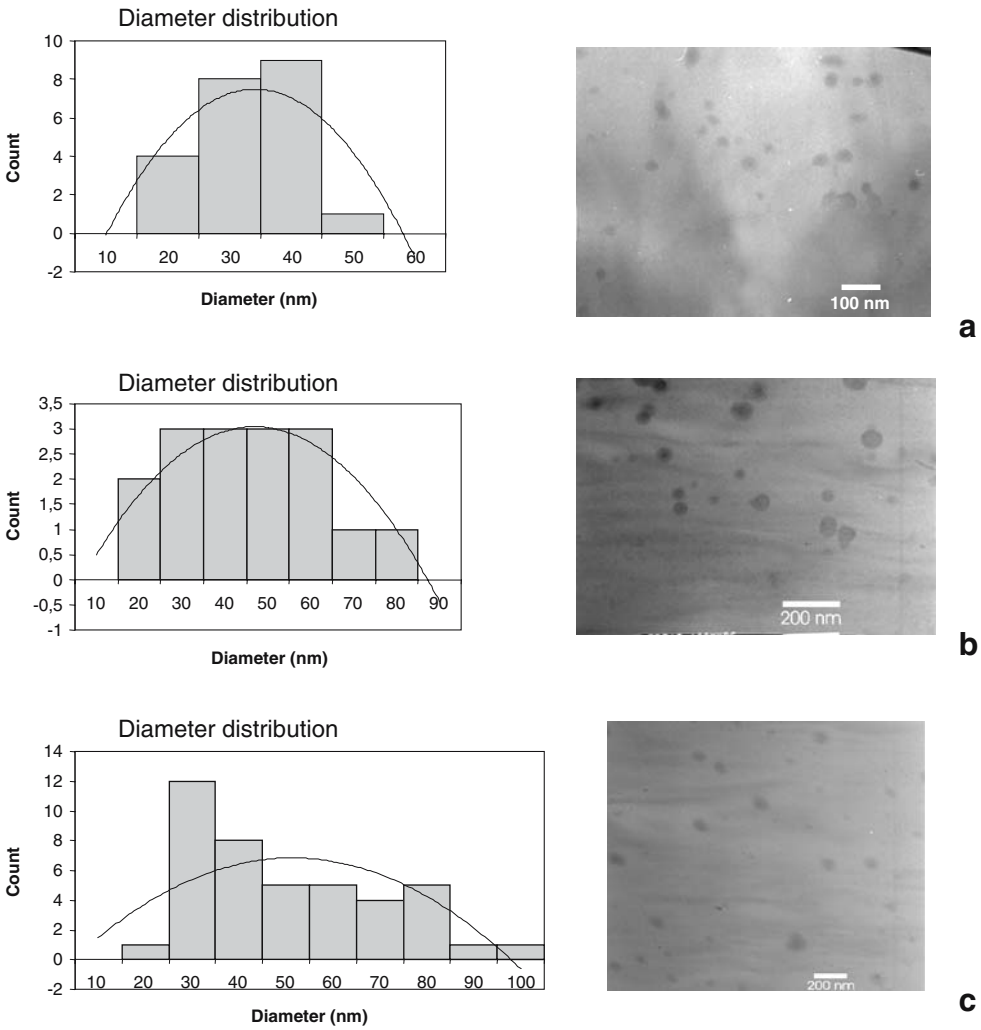


**Fig. 7** TEM micrographs and size distribution (histograms) of PGA nanoparticles cross-linked at 25 (**a**), 50 (**b**), and 100% (**c**)

SEC experiments of PGANPs were performed under similar conditions as were applied for PGA. The retention time values for PGANPs increase as the cross-linking degrees changes from 10 to 25%, and than with a smaller portion when increase from 50 to 100%. SEC traces of PGA and PGANPs at different ratio of cross-linking are compared in Fig. 5. The main peaks are related to the PGA and PGANPs, and the minor peak in the range of Rt = 15.1–16.8 min is unidentified impurity. The SEC traces demonstrate that unimodal PGANPs were obtained with a relatively narrow size distribution. We anticipate that larger particles formed by intermolecular reaction are disclosed by the filter system of SEC column. However, it was shown that the major component of PGANPs has a smaller hydrodynamic radius than that of the parent PGA.

Figure 6 shows the correlation of retention time and the cross-linking ratio. The calculated logarithmic curve gives the best fitting of the experimental values. In the SEC trace, the original PGA was observed at Rt = 8.757 min. Because of the cross-linking reactions, the retention time values increase, which might be interpreted as a decrease in the hydrodynamic volume of the cross-linked PGANPs. The shrinkage rate of nanoparticles was fitted by logarithmic plot. The cross-linkers built in the polymer chain act as constrains, which result a limited swelling of the nanoparticles; however, the particles remain water soluble.

*Particle size by TEM* It was shown that PGA and 10% cross-linked PGANPs can be prepared as a film; however, the cross-linked nanoparticles separated into spherical particles in an aqueous environment. TEM micrographs (Fig. 7) confirmed the nanosize of dried cross-linked PGA particles and show the distribution of these derivatives. The size of the dried particles varied in the range of 20–90 nm. Similar narrow size ranges can be observed in case of samples A, B, and C with different cross-linking ratio. The profile of dried cross-linked particles are rather flat particles understanding the pale objects with low thickness on TEM micrographs than in a swollen state, where spherical particles are expected to form. The histogram for the 100% cross-linked particles seems to indicate larger particles and a broader size distribution than at a low cross-linking ratio. In this case, the large amount of cross-linker and lower charge density of the polymer will probably lead to enhanced interpolymer cross-linking of adjacent chains and the formation of aggregates.

*Rheology* A large number of synthetic polyacrylic acid derivatives (Carbopol) are used as thickeners and mucoadhesives [37, 38]. Viscosity is an important property that is related to the nature and the extent of intermolecular interactions and entanglements in polymer systems. Figure 8 shows the shear rate dependence of the viscosity at various particle and polymer concentrations for PGA and PGANPs of different degrees of cross-linking. A virtually Newtonian behavior, over the considered shear rate domain, is observed for the PGANPs solutions at all levels of cross-linking. This finding and the low viscosities of these solutions indicate that no interconnected network structures are formed even at high

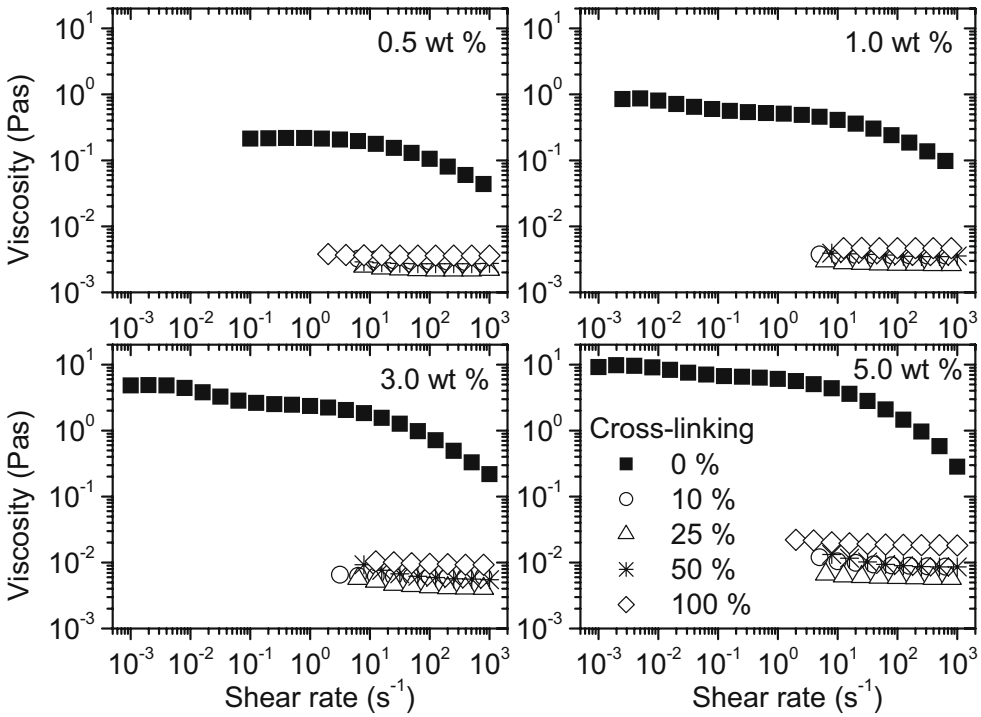


**Fig. 8** Shear rate dependence of the viscosity for the PGA and PGANPs systems at the indicated polymer concentrations and cross-linker densities

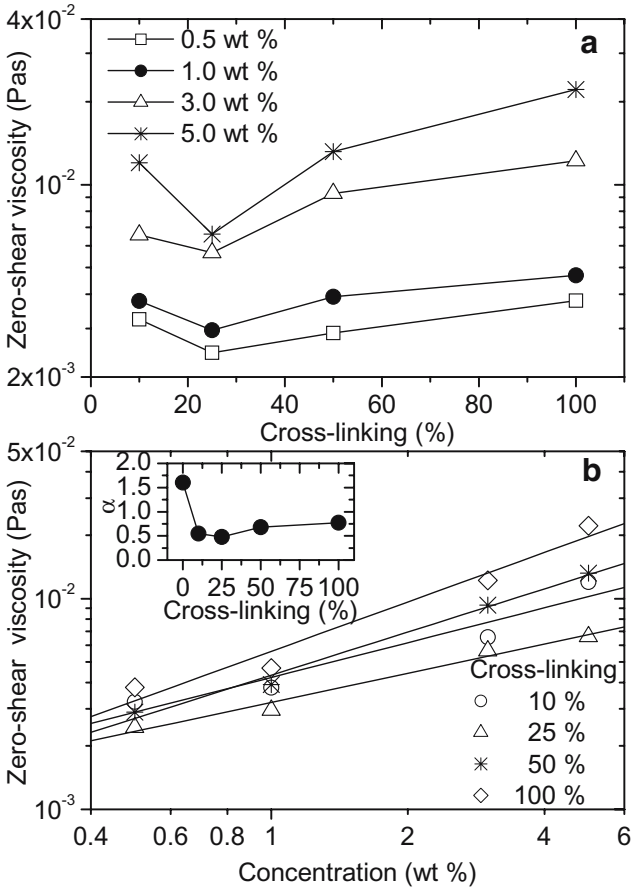


**Fig. 9** **a** Effect of cross-linking density on the zero-shear viscosity at the particle concentrations indicated. **b** Concentration dependence of the zero-shear viscosity at the given cross-linking densities. The *inset plot* shows the values of the exponent $\alpha$, expressing the concentration dependence of the zero-shear viscosity $(\eta_0 \sim c^{\alpha})$

polymer concentration, but there may still be a present interaction between particles or coils that have not been cross-linked. This is a typical rheological behavior [39] for systems containing compact particles. In contrast, the solutions of the parent linear PGA exhibit significantly higher viscosity and a gradually more pronounced shear-thinning effect at higher shear rates as the polymer concentration increases. This suggests polymer association and formation of entanglements in the solutions of PGA as the polymer concentration rises. The progressive decrease in viscosity as the shear rate rises is ascribed to the breakdown of the network junctions; that is, the rate of network disruption exceeds the rate at which associations are reformed. These features and the TEM results clearly support the hypothesis that the cross-linking process with EDBEA yields particles, and henceforth our attention will be focused on the effects of cross-linking and concentration of these particles on the physico-chemical properties of the system.

Effects of polymer concentration and degree of cross-linking on the zero-shear viscosity $\eta_0$ are depicted in Fig. 9a. The general trend that appears is that the zero-shear viscosity exhibits a minimum at a cross-linking density of 25%, followed by a rise in $\eta_0$ as the degree of cross-linking increases. These effects become more pronounced as the concentration of the particles rises. These features may be rationalized in the following scenario. When a low amount of cross-linker agent is added to the polymer solution, some of the PGA molecules have not been cross-linked, and they contribute to the viscosity more than the cross-linked particles. At higher cross-linker concentration, most of the PGA coils have been cross-linked, and the intrachain cross-linking process yields more compact particles and hence lower viscosity (viscosity minimum). At higher levels of cross-linker addition, the charge density of the polymer will decrease, and the probability for interchain cross-linking (two or more PGA chains are cross-linked to each other) increases, and the formed aggregates give rise to an increase in the value of $\eta_0$ as the cross-linker concentration rises. This effect is expected to become more dominant as the concentration of particles increases.

The concentration dependence of $\eta_0$ (see Fig. 9b) can be described by a power law $\eta_0 \sim c^{\alpha}$, where the value of $\alpha$ is displayed in the inset plot. The values of $\alpha$ are low, which is typical for systems where the intermolecular interactions are weak. However, it is evident from the inset that the value of $\alpha$ passes through a minimum at 25% cross-linker density, and a stronger concentration dependency of $\eta_0$ is detected at higher levels of cross-linking, which is expected when larger aggregates are evolved.

To gain some insight about the electrostatic interactions in the systems, we have added salt (NaCl) to screen the Coulombic forces (see Fig. 10) in 1-wt% solutions of PGANPs with different cross-linker concentration. It is obvious that the value of the zero-shear viscosity initially falls off strongly when salt is added, which indicates that

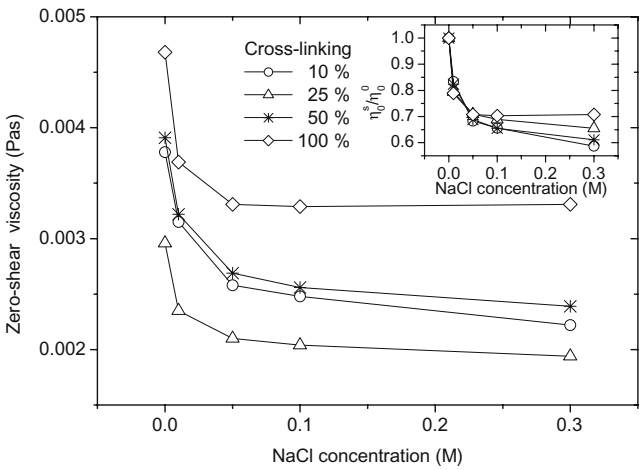


**Fig. 10** Effect of salt on the zero-shear viscosity at 1 wt% PGANP concentration at the cross-linker densities indicated. The *inset plot* shows the normalized viscosity as a function of salt concentration (see text for details)

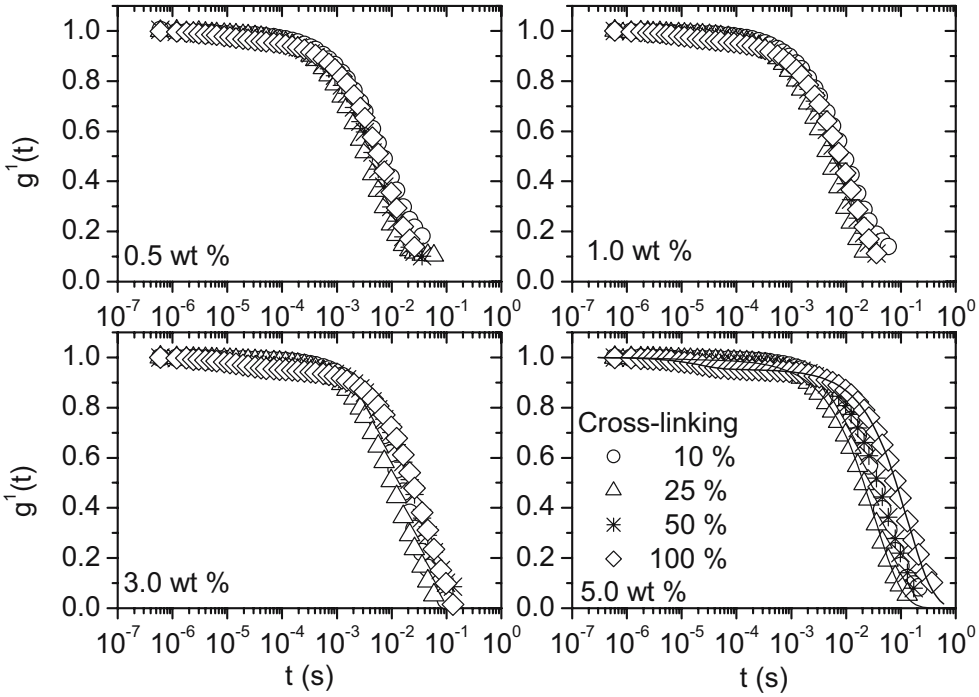


**Fig. 11** Plot of the first-order field correlation function versus time for the cross-linking densities and concentrations indicated at a scattering angle of 90°. The *solid curves* are fitted with the aid of Eq. 1

the species contract as the electrostatic interactions are screened. This finding stresses the importance of electrostatic interactions. For a close inspection of the salt effect, the inset shows a plot of the normalized viscosity $\eta_0^S/\eta_0^0$ (where $\eta_0^S$ is the zero-shear viscosity at the considered salt concentration and $\eta_0^0$ is that without added salt) against NaCl concentration for the studied cross-linker densities. This plot clearly illustrates that at the highest degree (100%) of cross-linking; the normalized zero-shear viscosity levels off at 0.05 M salt concentration, whereas at lower cross-linker densities, the screening of electrostatic interactions continues up to the highest considered salinity. This supports our conjecture that the electrostatic interactions are less dominant at higher levels of cross-linking. It is expected that a higher degree of cross-linking will lead to a diminution of the ionizable carboxyl groups per molecule.

*Dynamic light scattering* Figure 11 shows normalized time correlation function data, together with some curves fitted with the aid of Eq. 1, at a scattering angle of 90° for aqueous solutions of PGANPs of different degrees of cross-linking and concentration of particles. The correlation functions can always be well fitted by means of Eq. 1. The general picture that emerges is that the relaxation is slowed down as the particle concentration and the degree of cross-linking increase.

The mutual diffusion coefficient D for dilute polymer solutions can be expanded to first order in concentration as $D = D_o(1 + k_D c + \ldots)$, where $D_o$ is the diffusion coefficient at infinite dilution and $k_D$ determines the concentration dependence of $D$. To discuss particle dimensions, it is convenient to consider the hydrodynamic radius, which can be determined from the diffusion coefficient extrapolated to zero concentration by using the Stokes–Einstein relation: $R_h = kT/6\pi\eta D_o$, where $k$ is Boltzmann's constant, $T$ is the absolute temperature, and $\eta$ is the solvent viscosity. Because both the fast and the slow mode are diffusive at all conditions, the hydrodynamic radii of small ($R_{h,f}$) and large ($R_{h,s}$) particles can be determined via this relationship. The behaviors at different degrees of cross-linking are illustrated in Fig. 12. The results suggest that the system can be represented by a bimodal distribution of particle sizes; $R_{h,f}$ reflects some average size of single particles and

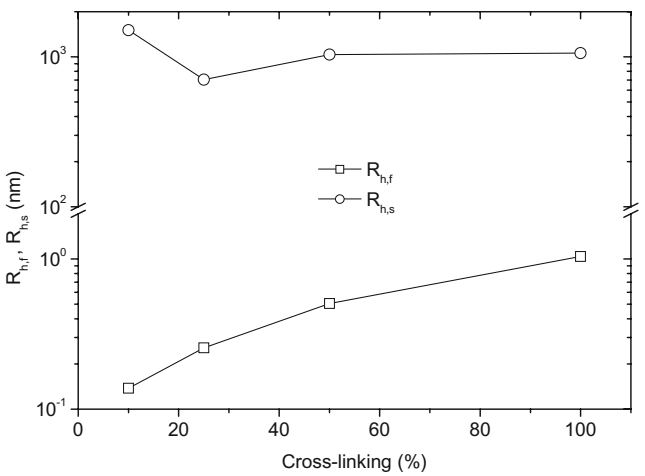


**Fig. 12** Effect of cross-linking density on the hydrodynamic radii for the fast ($R_{h,f}$) and the slow ($R_{h,s}$) mode, extrapolated to zero polymer concentration and calculated via the Stokes–Einstein relation

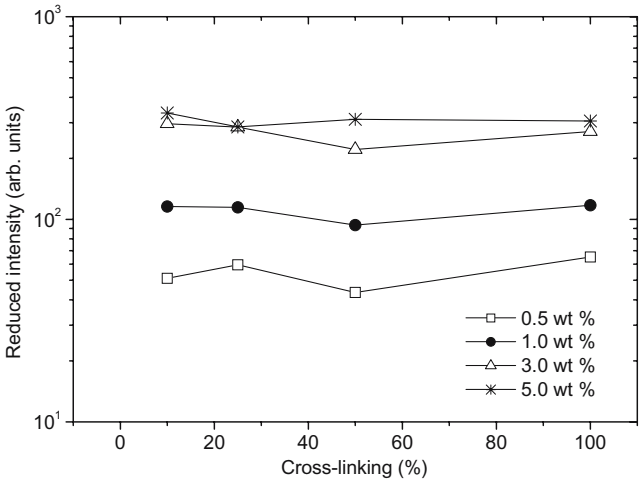


**Fig. 13** Effect of cross-linking density on the reduced intensity at 90° for the particle concentrations indicated

small aggregates, while $R_{h,s}$ yields the average size of larger clusters of particles (interpolymer cross-linked chains and/or large PGA coils) in the solution. The value of $R_{h,f}$ is small (≤1 nm) and increases with increasing cross-linker density, which probably reflects the contribution from some small aggregates. The reason for the absence of a minimum in the data of $R_{h,f}$ is probably that the incipient cross-linking of the PGA coils is not reflected in this population of small species.

The values of $R_{h,s}$ indicate that the solutions contain polymer species that are huge. The profile of the curve for $R_{h,s}$ reveals a similar behavior as observed for the viscosity. This indicates that the slow relaxation mode probes the incipient cross-linking of the PGA coils and at higher cross-linker concentrations the formation of large interpolymer complexes.

In Fig. 13, the reduced intensity (at a scattering angle of 90°) is plotted vs the cross-linker concentration for different particle concentrations. As expected, the value of the reduced intensity rises as the concentration of polymer species increases. However, it is interesting to note that the reduced intensity is virtually at all polymer concentrations independent of cross-linker density. This may suggest that at a low cross-linker concentration, the main contribution to the reduced intensity is the noncross-linked PGA coils, whereas at higher cross-linker densities, the shrinking of the entities because of intrachain cross-linking is compensated by the growth of interchain complexes.

Figure 14 shows the $q$ dependence of the reduced intensity $I_{red}$ for the polymer concentrations and cross-linker densities indicated. In the limited q range covered in these measurements, the wave vector dependence of $I_{red}$ can be described by a power law $I_{red} \sim q^{\mu}$, where the value of $\mu \cong 3$ may reflect that the species are compact and spherical. It is interesting to note that the value of the exponent does not vary with particle concentration or cross-linker density. This suggests that on the probed dimensional scale, the structure is compact and spherical-like also for the large interpolymer clusters. This work has demonstrated the omnipresent competition between intrachain and interchain behavior in these systems. In a previous study [39], it has been shown that the tendency to form interpolymer complexes during the cross-linking process can be reduced by applying a high shear rate on the sample during the cross-linker reaction.

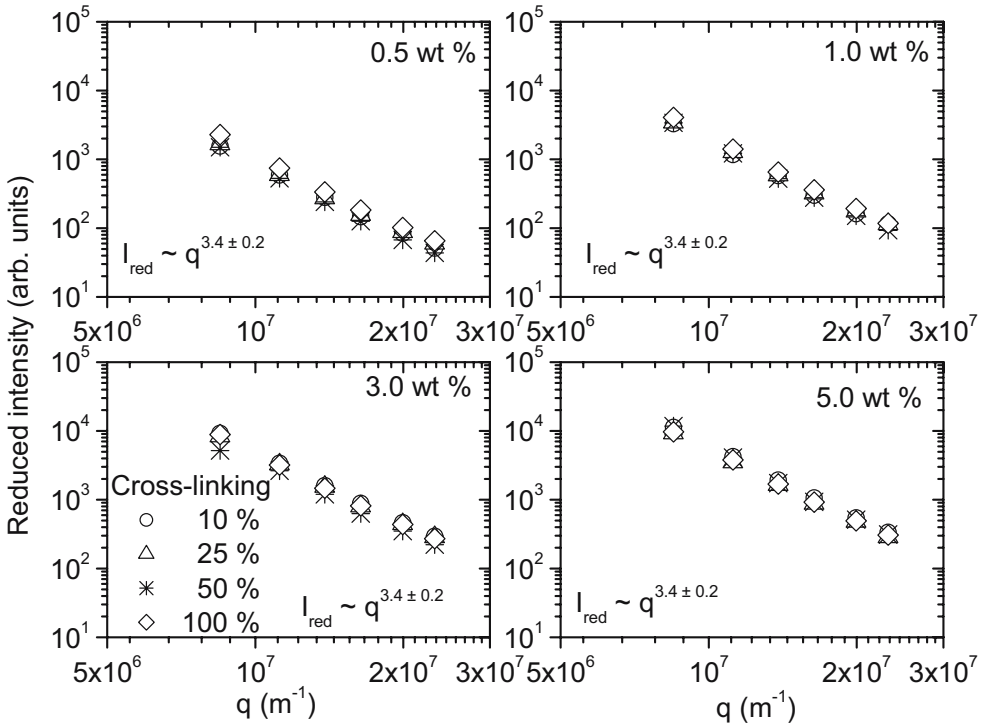


**Fig. 14** Wave vector dependence of the reduced intensity for the PGANPs concentrations and cross-linking densities indicated

## Conclusions

PGA was easily modified in aqueous solution by amidation with a bifunctional amine (EDBEA). Cross-linked nanoparticles (PGANPs) with different cross-linking ratios were prepared and characterized. The results from this study reveal that the size of the particles in the dry state (TEM) and in solution (SEC and dynamic light scattering [DLS]), as well as the rheological properties are all dependent on the relative amount of EDBEA incorporated into the PGANPs. Both TEM and DLS data suggest particles with broad size distributions. The cross-linked PGANPs have much lower viscosities than the parent PGA, probably because of contraction of the entities in connection with intrachain cross-linking of the molecules and the absence of entanglement couplings.

The DLS results indicate initially an exponential decay followed by a stretched exponential at longer times, and both relaxation modes are diffusive. The fast mode probes the diffusion of small particles, whereas the slow mode monitors the diffusion of large clusters.

The viscosity and DLS findings suggest an initial compression of the entities at low cross-linker ratios, followed by a growth of the species at higher cross-linker densities. The general picture that emerges is that at a low cross-linker ratio, not all PGA molecules are cross-linked, and they contribute to the augmented viscosity and hydrodynamic radius. At a low cross-linker density, most of the molecules have been cross-linked intramolecularly, and this sample contains mostly contracted molecules, giving rise to the minima observed in the viscosity and in $R_{h,s}$. At higher cross-linker ratios, the high amount of cross-linker agent and the reduction in the repulsive electrostatic forces give rise to interchain association and growth of aggregates.

The low viscosity of the PGANP solutions associated with the high specific surface because of the formation of particles make these PGANPs ideal candidates for drug delivery carriers. Entrapment of biologically active substances into the intramolecularly cross-linked network of these biodegradable molecules, followed by diffusion-driven slow release at specific sites, could lead to the development of new methods in medicine, pharmaceutics, and gene therapy.

**Acknowledgment** This work was supported by RET (Grant of Regional University Knowledge Center) contract numbers (RET-06/423/2004 and RET-06/432/2004) and in part by ElizaNor Polymer LLC, USA. B. N. gratefully acknowledges support from the Norwegian Research Council through a NANOMAT project (158550/431). Authors acknowledge the fermentation facilities of Dr. Levente Karaffa (Department of Genetics, University of Debrecen).

## References

1. Langer R, Tirrell DA (2004) Nature 428:487
2. Bastioli C (1998) Macromol Symp 135:193
3. Ivánovics G, Erdos LZ (1937) Immunitatsforschung 90:5
4. Kocianova S, Vuong C, Yao Y, Voyich JM, Fischer ER, DeLeo FR, Otto M (2005) J Clin Invest 115:688
5. Bovarnick M (1942) J Biol Chem 145:415
6. Kubota H, Nambu Y, Endo T (1993) J Polym Sci A Polym Chem 31:2877
7. Williams WJ, Thorne CB (1954) J Biol Chem 210:203
8. Zanuy D, Aleman C, Munoz-Guerra S (1998) Int J Biol Macromol 23:175
9. Xu H, Jiang M, Li H, Lu D, Quyang P (2005) Proc Biochem 40:519
10. Nagai T, Koguchi K, Ito Y (1997) J Agric Food Chem 46:891
11. Ashiuci M, Tani K, Soda K, Misono H (1999) J Biochem 123:1156
12. Hara T, Ueda S (1982) Agric Biol Chem 46:2275
13. Hara T, Fujio Y, Ueda S (1982) J Appl Biochem 4:112
14. Fan K, Gonzales D, Sevoian M (1996) J Environ Polym Degrad 4:253
15. Gonzales D, Fan K, Sevoian M (2000) J Polym Sci A Polym Chem 34:2019
16. Kunioka M (2004) Macromol Biosci 4:324
17. Obst M, Steinbuchel A (2004) Biomacromolecules 5:1166
18. Li C (2004) Adv Drug Deliv Rev 54:695
19. Shih IL, Van YT (2001) Biores Technol 79:207
20. Oppermann-Sanio FB, Steinbuchel A (2002) Naturwissenschaften 89:11
21. Shah DT, McCartly SP, Gross RA (1992) ACS Polym Prepr 33:488
22. Munoz-Guerra S, Melis J, Perey-Camero G, Bou JJ, Congregado F (1998) ACS Polym Prepr 39:138
23. Crescenzi V, D'Alani M, Palleschi C, Petragallo T (1994) ACS Polym Prepr 35:407
24. Borbely M, Nagasaki Y, Borbely J, Fan K, Bhogle A, Sevoian M (1994) Polym Bull 32:127
25. Melis J, Morillo M, Martinez de Ilarduja A, Munoz-Guerra S (2001) Polymer 42:9319
26. Kunioka M (1995) Appl Microbiol Biotechnol 44:501
27. Sidman KR, Schwope AD (1980) Membr Sci 7:277
28. Shih IL, Van YT, Chang YN (2002) Enzyme Microbial Technol 31:213
29. Krause WE, Bellomo EG, Colby RH (2001) Biomacromolecules 2:65
30. Starkweather ME, Muthukumar M, Hoagland DA (1999) Macromolecules 32:6837
31. Du G, Yang G, Qu Y, Chen J, Lun S (2005) Proc Biochem 40:2143
32. Thorne CB, Gomez CG, Noyes HE, Housewright RD (1954) J Bacteriol 68:307
33. Maleki A, Kjøniksen AL, Nyström B (2005) J Phys Chem B 109:12329
34. Kjøniksen AL, Nyström B, Lindman B (1998) Langmuir 14:5039
35. Lauten RA, Nyström B (2003) Colloids Surf A Physicochem Eng Asp 219:45
36. Nyström B, Thuresson K, Lindman B (1995) Langmuir 11:1994
37. Park H, Robinson JR (1987) Pharm Res 4:457
38. Riley RG, Smart JD, Tsibouklis J, Dettmar PW, Hampson F, Davis JA, Grant Kelly G, Wilber WR (2001) Int J Pharm 217:87
39. Kjøniksen AL, Laukkanen A, Galant C, Knudsen KD, Tenhu H, Nyström B (2005) Macromolecules 38:948